Dentomaxillofacial Radiology (2020) 49, 20190002

birpublications.org/dmfr

TECHNICAL REPORT

Selection and application of coils in temporomandibular joint MRI

[1]Qi Sun, [1]Min-jun Dong, [1]Xiao-feng Tao, [1]Meng-da Jiang and [2]Chi Yang

[1]Department of Radiology, Shanghai Ninth People's Hospital, Shanghai Jiao Tong University School of Medicine, Shanghai, China; [2]Department of Oral Surgery, Ninth People's Hospital, Shanghai Key Lab of Stomatology, Shanghai, China

Objective: To compare and evaluate the signal-to-noise ratio (SNR) and the contrast-to-noise ratio (CNR) values between a 15-channel phased array head coil and 6-channel dS Flex M surface coil in the MRI of temporomandibular joint.
Methods: 300 patients were randomly assigned to two groups: 150 patients were examined by using a 15-channel phased array head coil and the other 150 patients were scanned by using a 6-channel dS Flex M surface coil. All of the data were set in the same 6 regions of interest including the temporal lobe, condyle neck, lateral pterygoid muscle, parotid gland, the adipose area and an area of the background noise) . SNR and CNR values were measured respectively.
Results: The numerical variation law of SNR and CNR values measured in regionsof interest of each group was similar, although different coils were used. There were statistically significant differences of SNR values in all of the oblique sagittal (OSag) proton density-weighted imaging, the part of OSag T_2 weighted image (T_2WI) except for SNR_4 and SNR_5. and oblique coronal (OCor) T_2WI sequence except for SNR_2. On the contrary, SNR_4 and SNR_5 values in the OCor T_2WI and SNR_5 values in OSag T_2WI sequences by using the surface coil were higher than those by using the head coil. There were no statistically significant intergroup differences of CNR values in OSag proton density-weighted imaging sequence except CNR_1 and in OSag T_2WI sequence except CNR_5. But, statistically significant differences of all the values in the OCor T_2WI sequence except for CNR_1 were observed.
Conclusion: Both the phased array head coil and dS Flex M surface coil can be used for temporomandibular joint MRI.
Dentomaxillofacial Radiology (2020) **49**, 20190002. doi: 10.1259/dmfr.20190002

Cite this article as: Sun Q, Dong M, Tao X, Jiang M, Yang C. Selection and application of coils in temporomandibular joint MRI. *Dentomaxillofac Radiol* 2020; **49**: 20190002.

Keywords: temporomandibular joint; MRI; signal-to-noise ratio; contrast-to-noise ratio; coil

Introduction

Temporomandibular joint disorder (TMD), a collective term for the various pathologies of the temporomandibular joint (TMJ) and the masticatory muscles, is a common clinical disease.[1–4] TMD that often decreases the quality of life and causes great social economic costs is associated with a wide variety of frequent conditions such as tension, migraine headache, depression, fatigue, sleep apnea, obesity, and type II diabetes mellitus.[3–10] With the development of modern medical imaging, main auxiliary diagnostic methods for TMD are changing fast, including X-rays, arthrography, CT, and MRI; meanwhile, the studies and reports about TMJ imaging have been increasing.[2,4,6,7,11,12] It is well known that MRI is the golden-standard for non-invasive evaluation of TMJ because of the following characteristics: no X-ray radiation; clear display of the articular disc, retrodiscal tissue, soft-tissue structures, cartilage, and bone, particularly in cases of articular disc dislocation.[11] Currently, 3.0 T MRI scanners are widely used

Correspondence to: Min-jun Dong, E-mail: peter_dongmj@yeah.net; Xiao-feng Tao, E-mail: cjr.taoxiaofeng@vip.163.com

Received 28 December 2018; revised 04 August 2019; accepted 09 September 2019

The authors Min-jun Dong and Xiao-feng Tao contributed equally to the work.

Table 1 Acquisition parameters of the applied MR sequences were displayed.

Sequences	*Position*	***TRITE (ms)***	***FOV (mm)***	*Reconstruction Matrix*	***Thicknesslgap (mm)***	***Flip angle (°)***	*Slices*	*NSA*	*TA*	***Bandwidth (kHz)***
*T*2WI	Closed (OCor)	2500/70	110 × 110	384 × 224	1.5	90	16	2	2'13"	290.7
*T*2WI	Opened (OSag)	2500/65	110 × 110	384 × 224	2	90	16	2	2'07"	206.5
PDWI	Closed (OSag)	2000/20	110 × 110	400 × 256	2	90	16	2	2'05"	234.8

FOV, field of view; OCor, oblique coronal; OSag, oblique sagittal; PDWI, proton density-weighted image; TE, echo time; TR, repetition time; T_2WI, T_2 weighted image.

in the early screening and diagnosis of various clinical diseases. This approach not only obtains a high signal-to-noise ratio (SNR) and tissue resolution images but also improves the detection of small lesions.[13,14] SNR, an important quantity that is used to describe MRI system performance, is frequently used to evaluate images, measure contrast enhancement, assess sequence pulses, compare radiofrequency coils, and perform quality assurance, which is defined as the ratio by the signal of protons in the pixel and their noises.[13–15] Contrast-to-noise ratio (CNR) is defined as the ability to detect the differences of the different tissue components and also used as the indicator of image quality.[16] The larger the SNR and CNR values are, the better the image quality becomes. Meanwhile, how to select the most effective sequence for TMJ MR diagnosis in a limited time is of great significance. Stehling et al[12] and Schmid-Schwap et al[17] better visualized the anatomical structures and improved diagnostic accuracy in cases of anterior disc displacement by using a 3.0T MR scanner, respectively. Manloiu et al[2] also compared the imaging of TMJ MRI by using a standard TMJ surface coil and a head coil of a 3.0 T scanner. However, only the SNR of a phantom model and a few volunteers were measured in these studies, so the quantitative TMD measurements could not be determined. So far, only a few studies have investigated the technical aspects of TMJ imaging.[2,7,13,14] Our study aimed to compare and analyze the SNR and CNR by using the 15-channel phased array head coil and 6-channel dS FLEX M surface coil on MRI of TMJ, respectively.

Methods and material

Patients

Institutional review board approval of Shanghai Ninth People's Hospital Ethics Committee was obtained for this study.

From December 2016 to July 2019, 300 patients were randomly divided into 2 groups of 150 patients each: 66 males and 84 females with a mean age 38.03 ± 14.41 years underwent imaging with a 15-channel phased array head coil; and another 63 males and 87 females with a mean age 38.45 ± 14.48 years underwent imaging with a 6-channel dS Flex M surface coil. None of the patients had contraindications for MRI. The exclusion criteria were pregnancy and claustrophobia. Moreover, no patients had metal implants in the mouth, so no metal artifacts were encountered in the imaged areas. All patients with suspected TMD were diagnosed in the Department of Oral Surgery or Department of Orthodontics, while the postoperative patients and patients who needed orthodontic or orthognathic treatment were excluded.

In addition, patients younger than 16 years and older patients wearing dentures, as well as patients who did not co-operate well during the TMJ scanning were excluded. After scanning, the senior doctor judged whether the case was enrolled in the group (Second elimination) . The severe bone changes in the condyle and abnormal signal in the regionsof interest (ROIs) were also excluded.

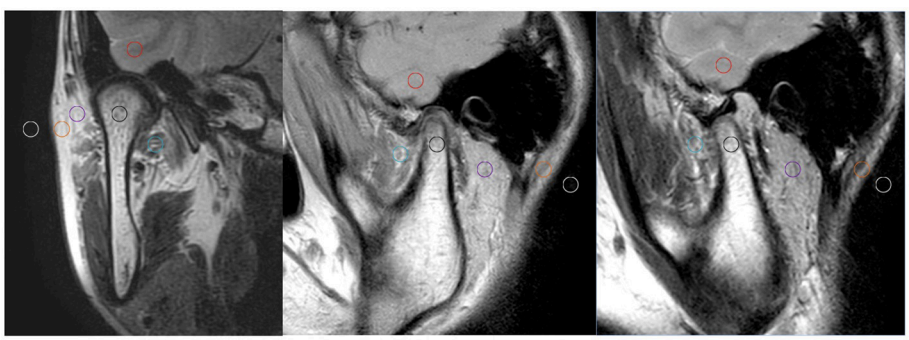

Figure 1 Six ROIs from 17 to 20 mm^2 in size were drawn on the median oblique sagittal and coronal position, respectively. ROI_1, temporal lobe (red circle); ROI_2, condylar neck (black); ROI_3, lateral pterygoid muscle, LPM (green); ROI_4, parotid gland (purple); ROI_5, adipose area (orange); and ROI6, the background noise (yellow). LPM,lateral pterygoid muscle; ROI, region of interest.

Table 2 Sex and age of the 300 patients included in the study

Type	*M*		*F*		
Group	*Sex (Cases)*	*Age (Years)*	*Sex (Cases)*	*Age (Years)*	*Age (Years)*
Head coil (150 cases)	66	39.83 ± 15.15	84	36.62 ± 13.72	38.03 ± 14.41
Surface coil (150 cases)	63	40.08 ± 14.90	87	37.28 ± 14.14	38.45 ± 14.48
p-value	-	>0.05	-	>0.05	>0.05

Scanning position and measurement method

All of the participants underwent MR scanning on a 3.0 T MR scanner (Ingenia, Philips Healthcare Systems, The Netherlands). Conventional MRI protocols that 300 patients underwent were used, and the main scanning parameters of sequences are shown in Table 1. All patients underwent simultaneous bilateral scanning of TMJ: proton density-weighted imaging (PDWI) sequences were acquired in oblique sagittal (OSag) planes with a closed mouth; T_2 weighted images (T_2WI) were acquired in oblique coronal (OCor) planes with a closed mouth; and T_2WI were acquired in OSag planes with an open mouth (with auxiliary opening fixation device).

The patients lay in the headfirst supine position; the scanning range included the entire TMJ region (disc–condyle complex) and the surrounding muscle tissue. The surface coils were adjusted to the center of the bilateral TMJ close to the surface of the joint and fixed with a soft cloth or bandage.[12,18] The head coil requires no adjustment, and the patients' shoulders reached the bottom of the coil without the auxiliary fixation device. Based on the axial position, the condyle head could be displayed clearly and the oblique sagittal location lines in the closed mouth position were perpendicular to the long axis of the condyle head; the oblique sagittal position of opening mouth should be adjusted according to the actual opening location.

Five ROIs from 17 to 20 mm^2 in size (ROI_1, temporal lobe; ROI_2, condylar neck; ROI_3, lateral pterygoid muscle, LPM; ROI_4, parotid gland; and ROI_5, adipose area) and one ROI of the background noise were selected and drawn on the median oblique sagittal and coronal position, respectively (Figure 1). The calculation formulae for SNR and CNR were as follows:

$SNR_n = S_n/\sigma$ (n = 1, 2, 3, 4, 5)[14,15,19–21]

$CNR_\triangle = |S_\triangle - S_3|/\sigma$ ($\triangle$ = 1,2,4,5)[22,23]

σ: standard deviation (SD) of the background noise

S_n, $S_\triangle$: mean signal intensity (SI)

S_3: mean SI of the lateral pterygoid muscle

Statistical analysis

The anonymized MR images of each patient were sorted in a random order. Two senior radiologists analyzed the images using a double-blind method. The clarity of the anatomical structures was rated from 1 to 5 according to a previously published grading system[1,3,5] : 1, not visible and impossible to diagnose; 2, poor visibility with more motion artifacts affecting the diagnosis; 3, moderate visibility with a small amount of motion artifact but not affect the diagnosis; 4, good visibility with little motion artifact; and 5, excellent visibility and clear contours with no artifacts.

SPSS® software v. 21.0 (IBM Corp., New York, NY; formerly SPSS Inc., Chicago, IL, USA) was used for the statistical analyses. The SNR and CNR values of each group were compared and calculated on a workstation (Ingenia Extended WorkStation; Philips Healthcare Systems). All of the data were compared on the same display (24-inch widescreen LCD monitor, 1920 × 1200 pixels, 74.04 Horz Freq [kHz], 60 Vert Freq [Hz]; Hewlett-Packard Development Company, L.P., Palo Alto). The results were statistically analyzed using the independent sample t-test. Values of $p < 0.05$ were considered statistically significant. To determine the inter-reader agreement on the qualitative MRI analysis, κ statistics was used. κ values of 0.41–0.60 were considered moderate agreement, 0.61–0.80 were considered substantial, 0.81–0.99 were considered almost perfect, and 1.00 was considered perfect.

Table 3 Temporomandibular joint disorders included in the study

Type	*TMDs (cases)*		
Group	*By head coil*	*By surface coil*	*Total*
Single R	19	22	41
Single L	35	35	70
Bilateral	70	67	137
Neither	25	27	52
Total	150	150	300

TMD, temporomandibular joint disorder.

Results

There was no significant intergroup difference between the 300 patients in sex or age (Table 2) ($p > 0.05$). Among the 300 cases, 52 had a bilateral normal disc–condyle complex relationship; 137 had bilateral TMD; 41 were diagnosed as right TMD; and 70 were diagnosed as left TMD. The MRI diagnosis positive rate of TMD was 82.67% (Table 3). Among 600 sides, 138 cases of unilateral TMJ were found with simple joint noise or

Table 4 Distribution of clinical symptoms was as follows

	Phase array coil (150 cases) *		*Surface coil (150 cases)* *	
	R # *(150 sides)*	*L* # *(150 sides)*	*R* # *(150 sides)*	*L*# *(150 sides)*
Joint noise/ snapping (Single)	34	35	33	36
Limitation of mouth opening (Single)	35	37	36	36
Facial discomfort with pain (Single)	28	23	27	27
Two symptoms	43	47	45	42
All symptoms	10	8	9	9
Total	150	150	150	150
p	#$p > 0.05$		*$p > 0.05$	

snapping, 144 sides with limited mouth opening, 105 sides with facial discomfort, 177 sides with 2 symptoms, and 36 sides with 3 symptoms (Table 4). There were no statistically significant intergroup differences (phased array head coil and surface coil by R and L sides, respectively; $p > 0.05$).

Good or excellent agreement was found for SNR and CNR measurements and anatomical structure clarity between the two radiologists (intraclass correlation coefficient, 0.79–0.95). No statistically significant difference in SNR and CNR could be observed between the left and right sides in the same patient by using the same coil (Tables 5 and 6). In each group, the variation of SNR and CNR values measured from five ROIs were similar, although different coils and sequences were used. The SNR values were sorted from large to small as follows: $SNR_5 > SNR_4 \geq SNR_2 > SNR_1 > SNR_3$; Similarly, the CNR values were as follows: $CNR_5 > CNR_4 \geq CNR_2 > CNR_1$ (Figures 2 and 3).

Comparison of SNR values

The value of SNR_3 was the lowest in both coils; and the value by using the surface coil was lower. There were statistically significant differences of SNR values in all of the OSag PDWI and the part of OSag T_2WI sequence except for SNR_4 and SNR_5. Similarly, statistically significant differences of SNR values in OCor T_2WI sequence except for SNR_2 were also observed. On the contrary, SNR_4 and SNR_5 values in the OCor T_2WI and SNR_5 values in OSag T_2WI sequences by using the surface coil were higher than those by using the head coil (Figure 2, Table 5).

Comparison of CNR values

The lowest CNR value was CNR_1; and there were no statistically significant intergroup differences of CNR values in OSag PDWI sequence except $CNR_1$and in OSag T_2WI sequence except CNR_5. But, statistically significant differences of all the values in the OCor T_2WI sequence except for CNR_1 were observed (Figure 3, Table 6).

The images by using these two coils were obtained to meet the requirements of the imaging diagnosis (Table 7). Among them, the average score in the group by using head coil was 4.20 ± 0.80, and the average score in the group by using the surface coil was 4.4 ± 0.81. And there was significant difference between two groups ($p < 0.01$). 126 (84%) and 132 (88%) cases were more than Grade 3 by using the different coils in two groups respectively. The number of Grade 5 images by using the flex coil was higher than that by using the head coil, but there was no significant intergroup difference in the total number from Grade 3 to 5 images. Neither group had one score case.

Table 5 SNR measured left (L) and right (R) in five ROIs using different MR sequences with head (H) and surface (S) coil

Group	*Closed-mouth (R)*		*Opened-mouth (R)*	*Closed-mouth (L)*		*Opened- mouth (L)*	*P*值
SNR	*OSag PDWI*	*OCor* T_2*WI*	*OSag* T_2*WI*	*OSag PDWI*	*OCor* T_2*WI*	*OSag* T_2*WI*	*(H-S)*
SNR1 (H)	76.89 ± 6.09	76.45 ± 11.61	61.99 ± 8.02	77.01 ± 6.22	77.49 ± 10.26	61.63 ± 9.02	$p < 0.05$
SNR1 (S)	62.14 ± 7.95	71.11 ± 11.21	56.11 ± 14.86	59.25 ± 6.98	71.54 ± 11.07	55.13 ± 14.95	
SNR2 (H)	84.87 ± 10.37	80.82 ± 11.04+	71.52 ± 12.45	83.89 ± 9.66	80.96 ± 10.69+	71.65 ± 12.94	+$p > 0.05$
SNR2 (S)	71.54 ± 6.45	79.62 ± 11.24+	65.92 ± 7.04	70.67 ± 5.93	79.99 ± 11.55+	65.35 ± 8.22	
SNR3 (H)	49.61 ± 9.90	48.83 ± 9.01	33.84 ± 9.99	49.65 ± 8.02	49.03 ± 9.13	33.96 ± 7.01	$p < 0.05$
SNR3 (S)	37.99 ± 6.92	35.03 ± 8.97	24.84 ± 7.36	37.59 ± 7.03	35.76 ± 9.23	25.01 ± 7.13	
SNR4 (H)	86.92 ± 7.52	105.02 ± 14.02	70.47 ± 12.51*	87.01 ± 7.89	104.96 ± 13.76	70.84 ± 13.72*	*$p > 0.05$
SNR4 (S)	74.85 ± 6.35	115.12 ± 10.43	68.59 ± 6.16*	75.12 ± 5.94	115.28 ± 9.95	68.87 ± 6.72*	
SNR5 (H)	97.54 ± 6.97	153.56 ± 15.44	85.62 ± 14.36#	97.23 ± 6.75	154.01 ± 13.21	85.19 ± 14.73#	#$p > 0.05$
SNR5 (S)	89.44 ± 9.19	177.43 ± 11.13	87.43 ± 10.72#	87.99 ± 6.58	177.92 ± 11.98	87.05 ± 10.97#	
P值(R-L)	-	-	-	$p > 0.05$	$p > 0.05$	$p > 0.05$	-

OCor, oblique coronal; OSag, oblique sagittal; PDWI, proton density-weighted imaging; ROI, region of interest; SNR, signal-to-noise ratio; T_2WI, T_2 weighted image.

Table 6 CNR measured left (L) and right (R) using different MR sequences with head (H) and surface (S) coil

Group	*Closed-mouth (R)*		*Opened-mouth (R)*	*Closed-mouth (L)*		*Opened-mouth (L)*	p值
CNR	*Sag PDWI*	*Cor* T_2*WI*	*Sag* T_2*WI*	*Sag PDWI*	*Cor* T_2*WI*	*Sag* T_2*WI*	*(H-S)*
CNR1 (H)	1.69 ± 0.28^{+}	3.84 ± 1.01	1.97 ± 0.65	1.64 ± 0.31^{+}	3.83 ± 1.19	1.98 ± 0.56	$p^{+} < 0.05$
CNR1 (S)	1.50 ± 0.35	3.87 ± 1.53	2.02 ± 0.63	1.51 ± 0.39^{+}	3.88 ± 1.21	2.01 ± 0.88	
CNR2 (H)	2.31 ± 0.80	4.12 ± 1.19$^{\#}$	2.69 ± 0.84	2.32 ± 0.64	4.15 ± 1.32$^{\#}$	2.70 ± 0.81	$p^{\#} < 0.05$
CNR2 (S)	2.28 ± 0.55	5.59 ± 1.66$^{\#}$	2.73 ± 0.54	2.28 ± 0.49	5.58 ± 1.52$^{\#}$	2.76 ± 0.53	
CNR4 (H)	2.48 ± 0.72	6.91 ± 1.63$^{\&}$	2.65 ± 0.76	2.47 ± 0.57	7.02 ± 1.57$^{\&}$	2.67 ± 0.63	$p^{\&} < 0.05$
CNR4 (S)	2.43 ± 0.70	9.95 ± 1.71$^{\&}$	2.79 ± 0.67	2.45 ± 0.45	10.01 ± 1.62$^{\&}$	2.80 ± 0.61	
CNR5 (H)	3.30 ± 1.02	13.13 ± 2.06*	2.34 ± 1.34*	3.30 ± 0.91	13.09 ± 1.91*	3.36 ± 1.23*	$p^{*} < 0.05$
CNR5 (S)	3.36 ± 0.81	17.85 ± 2.02*	4.24 ± 0.87*	3.31 ± 0.68	17.83 ± 2.03*	4.25 ± 0.85*	
P值(R-L)	-	-	-	$p > 0.05$	$p > 0.05$	$p > 0.05$	-

CNR, contrast-to-noise ratio; PDWI, proton density-weighted imaging; T_2WI, T_2 weighted image.

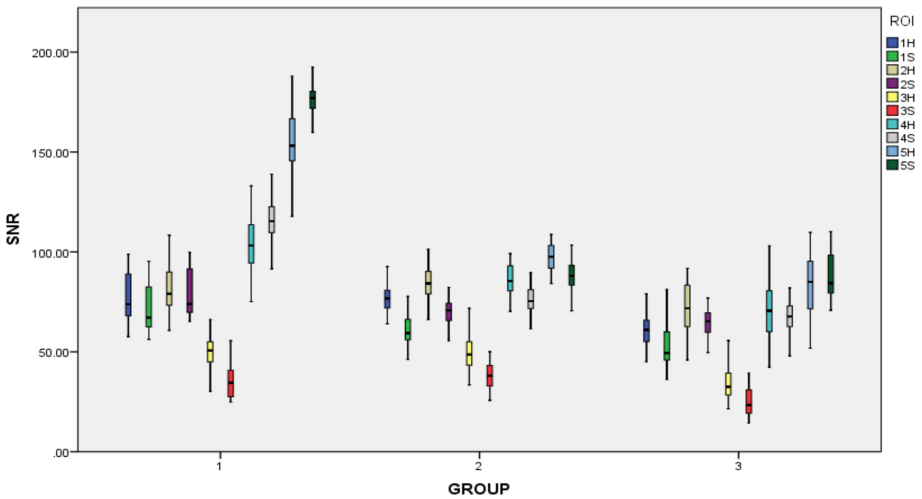

Figure 2 Box plot of SNR in five ROI with head (H) and surface (S) coil. In this box plot, the value of SNR_3 was the lowest in both coils, especially for the group of SNR_{3S} (red color). The value of SNR_5 was highest, especially for the group of SNR_{5S} (deep green color) because surface coil was nearest the subcutaneous fat. Group 1: group by using OCor T_2WI sequence with closed mouth. Group 2: group by using OSag PDWI sequence with closed mouth. Group 3: group by using OSag T_2WI sequence with opened mouth. OCor,oblique coronal; OSag, oblique sagittal; PDWI, proton density-weighted imaging;ROI, region of interest; SNR, signal-to-noiseratio; T_2WI, T_2 weighted image.

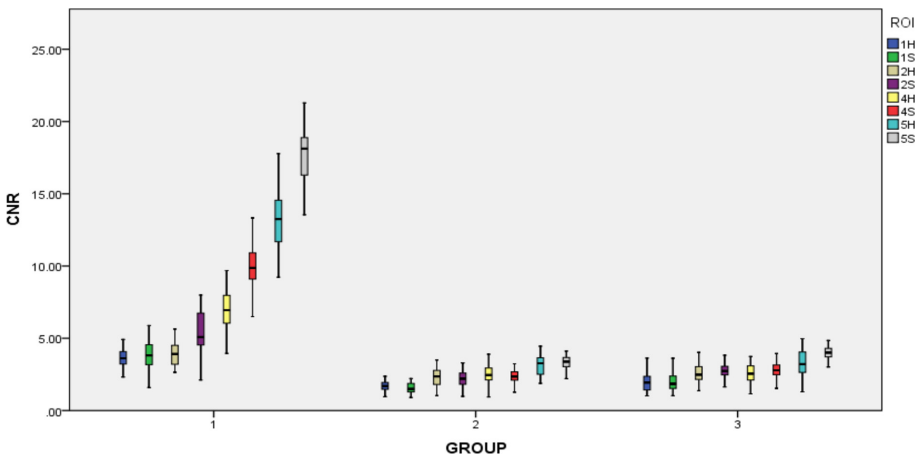

Figure 3 Box plot of CNR in five ROI with head (H) and surface (S) coil. In the box plot of CNR, the variation of CNR values measured in five ROIs between Group 2 and Group 3 were similar. In the Group 1, CNR values changed greatly from CNR_1 to CNR_5 by a stepped rise. The CNR value of ROI_{5S} in the Group 1 was highest. CNR,contrast-to-noise ratio; ROI, region of interest.

Table 7 The clarity of the anatomical structures was rated

	Type		
Score	*Head coil*	*Surface coil*	*Total*
5	60	90	150
4	66	42	108
3	18	12	30
2	6	6	12
1	0	0	0
Total	150	150	300

Discussion

The radiofrequency coil is an essential component of the MRI system. MRI scanning requires the coil to display the location and the structure of disease clearly.[24] The function of the RF coil is to transmit RF pulses and receive the MRI signals. RF coils can be divided into orthogonal, phased array, surface flexible, intraoperative, and array types.[25] The selection and reasonable application of the RF coil are the most important components. The phased array coils are composed of multiple single coils, which can provide more detailed MRI information for the inspected position. The soft surface coil is used to cover a limited area of the body during MRI, which can use the structure's characteristics to bring the coil as close to the detected position as possible to improve image quality.[16,24] In our study, the head coil that consists of a basilar coil and its upper coil is a phased array coil[25,26]; it is equipped with a supporting platform with a built-in rear coil for the head examination (30 cm, 15 channels). The dS Flex surface coil, which is mainly used for imaging small joints and limited regions, is a loop coil with a pedestal on the bottom and an annular integrated flex coil. It can be divided into small (10 cm, 4 channels), middle (15 cm, 6 channels), and large (20 cm, 8 channels) model that can clearly show the joint anatomy and lesions in small field of view imaging.

Most hospitals are currently equipped with a head coil but not the special TMJ surface coils. It is generally believed that surface coil can ensure a higher SNR by reducing the imaging range and depth.[27] Here we compared the SNR and CNR by using a 15-channel phased-array coil and the 6-channel dS Flex M surface coil on a 3.0 T MRI to identify the best coil for diagnosing TMJ disease. One investigation evaluated the MRI image quality of different protocols at 1.5 and 3.0 T and concluded that the increased image quality and higher CNR were associated with the higher SNR due to increased magnetic field strength.[28] Manloiu A et al found that the 32-channel head coil yielded a more accurate representation of TMJ structures, including the articular disc, bilaminar zone, and lateral pterygoid muscle for the volunteers.[2] However, another study reported that the imaging spatial resolution and positive detection rate of lesions of the multichannel phased array head coil were lower than those of the surface coil.[29] In this experiment, from the aspects of coil structure, design, and characteristics, the closer the surface coil was to the skin's surface, the stronger the signal was; also, a higher SNR can be obtained under the same scanning conditions. However, with increases in vertical depth, the SNR decreases of the surface coil were more obvious than those of the head phased array coil (SNR_3). Most SNR values of the 15-channel phased array head coil were higher than those of the 6-channel dS Flex M surface coil on the Philips Ingenia 3.0 T MRI (all but SNR_4 and SNR_5 in OSag T_2WI and SNR_2 in OCor T_2WI). Due to the difference in the inherent physical properties between the surface and head phased array coils, the values of SNR_4 and SNR_5 in OCor T_2WI and SNR_5 in OSag T_2WI sequences were higher using the surface coil than using the head coil. We also found that the comparison results of CNR values were opposite on the PDWI and OCor T_2WI sequences. All of the CNR values of the surface coils were higher than those of phased array coils on the OCor T_2WI and OSag T_2WI sequences. On the OSag PDWI sequence, the results were opposite except for CNR_5, but there was no significant intergroup difference in the imaging diagnostic rates in our study. The cause of the different results between our and other studies may be due to differences in machinery and coil structure; and differences in study populations.

In our experience, the dS Flex M surface coil can be used for routine clinic scanning and satisfy the need for the regular imaging diagnosis (Figure 4) . The disc–condylar complex relationship can be displayed clearly in less than 8 min. However, in cases of neoplastic lesions in the TMJ region or the need for diffusion, dynamic, or three-dimensional imaging sequencing, the head or neck phased array coil (according to the specific lesion location) should be selected (Figure 5). Moreover, we also studied another group of patients (not included in the study) for whom an MRI of the TMJ was performed immediately post-operatively and learned that 19 of 30 patients considered the phased array head coil more comfortable, while the others felt no significant difference between the two coils; and 13 of 30 patients felt pressure pain in the operative area induced by the dS Flex M surface coil since it required placement close to the skin to ensure extra fixation. With the post-operative dressing fixation in the TMJ region, the surface coil could not completely get close to the surface skin of the lesion, which affected the SNR and CNR values. In this study, we found another interesting phenomenon: The pre-scanning time using the phased array head coil was longer than that using the surface coil. Each sequence was 10–15 s depending on the patient's condition. This may be related to the number of channels of the coil because the higher the number of channels involved, the longer the time needed to draw sensitive maps.

This study has some limitations. First, greater sample sizes should be included in future studies. Second, the

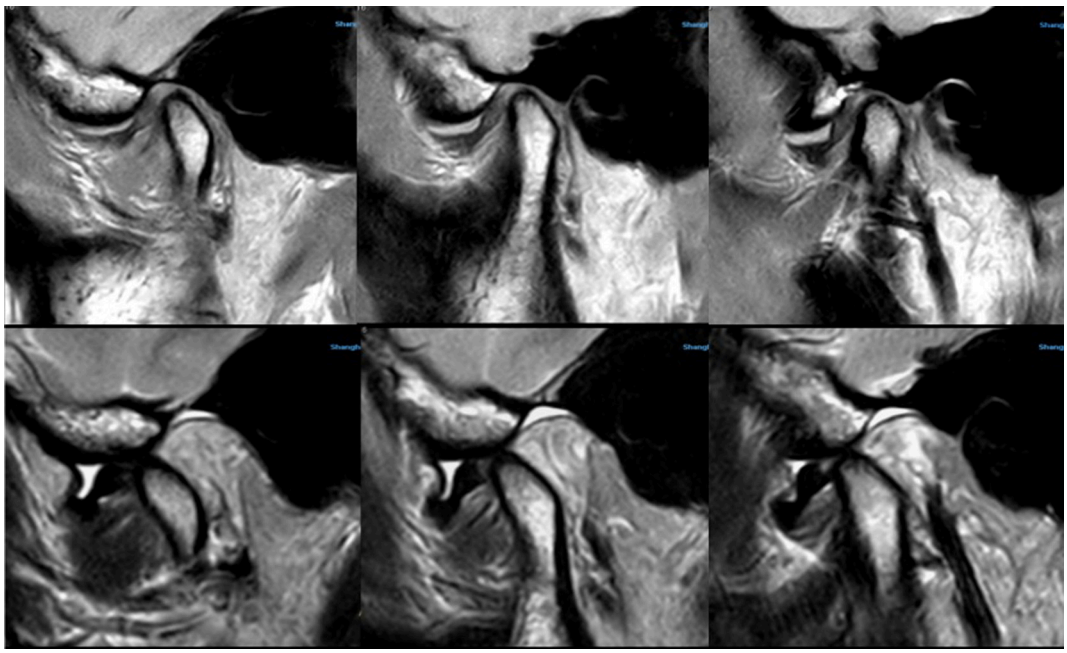

Figure 4 It clearly showed the relationship between articular disc and condyle by using Surface coil. TMJ MRI showed anterior disc displacement without reduction and medium amount of effusion in the upper articular cavity, which were obtained by the surface coil (Upper images were OSag PDWI with closed mouth, lower images were OSag T_2WI with opened mouth). The surface coil has better contrast although the signal decays very fast with the increasing in the depth of object, which can make the disc–condyle complex displayed clearly. OSag,oblique sagittal; T_2WI, T_2 weighted image; TMJ, temporomandibular joint.

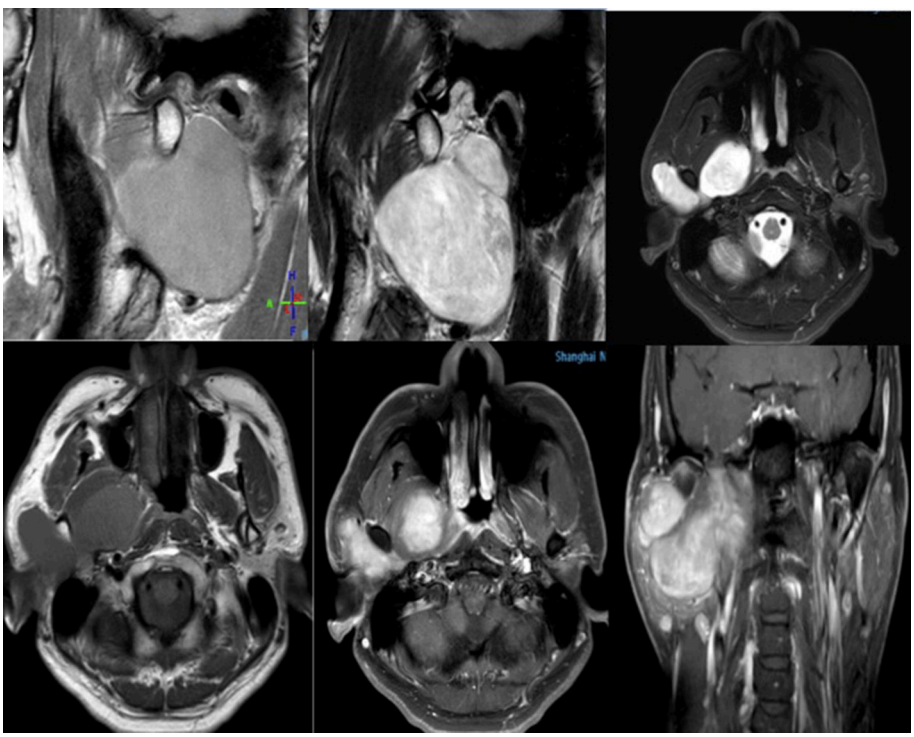

Figure 5 This is a patient with pain and swelling in the temporomandibular joint area. During the scanning, we found that it was a giant mass of parotid gland involving the temporomandibular joint area. Phased array coil has high signal-to-noise ratio and uniformity, and it can support a larger and longer scanning range; moreover, it is also very clear for displaying the structure of deep tissue.

researched types of diseases in this sample were relatively simple, so the results need to be further improved. Third, we did not assess patients with metal implants. Of course, we only compared SNR and CNR values of the two coils on the Philips Ingenia 3.0 T MRI scanner; further research is required to determine whether the same results can be obtained on other machines. Therefore, a more objective evaluation is needed to improve the imaging quality of TMJ MRI in future studies.

In summary, head and surface coils can both be used for TMJ MRI. We suggest that the surface coil can be used in the conventional TMJ imaging and the phased array head coil can be used for routine postoperative examinations or dynamic imaging. Further meticulous research is needed for its application to specific diseases. In the actual clinical setting, the particular coil should be chosen reasonably and correctly based on the disease location, lesion size, and diagnosis to improve image quality and diagnostic accuracy on MRI examinations.

References

1. Dym H, Israel H. Diagnosis and treatment of temporomandibular disorders. *Dent Clin North Am* 2012; **56**: 149–61. doi: https://doi.org/10.1016/j.cden.2011.08.002
2. Manoliu A, Spinner G, Wyss M, Filli L, Erni S, Ettlin DA, et al. Comparison of a 32-channel head coil and a 2-channel surface coil for MR imaging of the temporomandibular joint at 3.0 tesla. *Dentomaxillofac Radiol* 2016; **45**: 20150420. doi: https://doi.org/10.1259/dmfr.20150420
3. Wiechiewicz M, Boening K, Wiland P, Shiau YY, Paradowska-Stolarz A. Reported concepts for the treatment modalities and pain management of temporomandibular disorders. *J Headache Pain* 2015; **16**: 106. doi: https://doi.org/10.1186/s10194-015-0586-5
4. Eberhard L, Giannakopoulos NN, Rohde S, Schmitter M. Temporomandibular joint (TMJ) disc position in patients with TMJ pain assessed by coronal MRI. *Dentomaxillofac Radiol* 2013; **42**: 20120199. doi: https://doi.org/10.1259/dmfr.20120199
5. Kaimal S, Ahmad M, Kang W, Nixdorf D, Schiffman EL. Diagnostic accuracy of panoramic radiography and MRI for detecting signs of TMJ degenerative joint disease. *Gen Dent* 2018; **66**: 34–40.
6. Kayipmaz S, Akçay S, Sezgin Ömer Said, Çandirli C. Trabecular structural changes in the mandibular condyle caused by degenerative osteoarthritis: a comparative study by cone-beam computed tomography imaging. *Oral Radiol* 2019; **35**: 51–8. doi: https://doi.org/10.1007/s11282-018-0324-1
7. Manoliu A, Spinner G, Wyss M, Erni S, Ettlin DA, Nanz D, et al. Quantitative and qualitative comparison of MR imaging of the temporomandibular joint at 1.5 and 3.0T using an optimized high-resolution protocol. *Dentomaxillofac Radiol* 2016; **45**: 20150240. doi: https://doi.org/10.1259/dmfr.20150240
8. De Rossi SS. Orofacial pain: a primer. *Dent Clin North Am* 2013; **57**: 383–92. doi: https://doi.org/10.1016/j.cden.2013.04.001
9. Breckons M, Bissett SM, Exley C, Araujo-Soares V, Durham J. Care pathways in persistent orofacial pain: qualitative evidence from the deep study. *JDR Clin Trans Res* 2017; **2**: 48–57. doi: https://doi.org/10.1177/2380084416679648
10. Manfredini D, Guarda-Nardini L, Winocur E, Piccotti F, Ahlberg J, Lobbezoo F. Research diagnostic criteria for temporomandibular disorders: a systematic review of axis I epidemiologic findings. *Oral Surg Oral Med Oral Pathol Oral Radiol Endod* 2011; **112**: 453–62. doi: https://doi.org/10.1016/j.tripleo.2011.04.021
11. Shen P, Sun Q, Xu W, Zhen J, Zhang S, Yang C. The fate of autogenous free fat grafts in the human temporomandibular joint using magnetic resonance imaging. *J Craniomaxillofac Surg* 2015; **43**: 1804–8. doi: https://doi.org/10.1016/j.jcms.2015.08.024
12. Stehling C, Vieth V, Bachmann R, Nassenstein I, Kugel H, Kooijman H, et al. High-resolution magnetic resonance imaging of the temporomandibular joint: image quality at 1.5 and 3.0 Tesla in volunteers. *Invest Radiol* 2007; **42**: 428–34. doi: https://doi.org/10.1097/01.rli.0000262081.23997.6b
13. Wiens CN, Kisch SJ, Willig-Onwuachi JD, McKenzie CA. Computationally rapid method of estimating signal-to-noise ratio for phased array image reconstructions. *Magn Reson Med* 2011; **66**: 1192–7. doi: https://doi.org/10.1002/mrm.22893
14. Dietrich O, Raya JG, Reeder SB, Reiser MF, Schoenberg SO. Measurement of signal-to-noise ratios in MR images: influence of multichannel coils, parallel imaging, and reconstruction filters. *J Magn Reson Imaging* 2007; **26**: 375–85. doi: https://doi.org/10.1002/jmri.20969
15. Fleischer CC, Zhong X, Mao H. Effects of proximity and noise level of phased array coil elements on overall signal-to-noise in parallel MR spectroscopy. *Magn Reson Imaging* 2018; **47**: 125–30. doi: https://doi.org/10.1016/j.mri.2017.12.001
16. Hess R, Neitzel U. Optimizing image quality and dose for digital radiography of distal pediatric extremities using the contrast-to-noise ratio. *Rofo* 2012; **184**: 643–9. doi: https://doi.org/10.1055/s-0032-1312727
17. Schmid-Schwap M, Drahanowsky W, Bristela M, Kundi M, Piehslinger E, Robinson S. Diagnosis of temporomandibular dysfunction syndrome–image quality at 1.5 and 3.0 Tesla magnetic resonance imaging. *Eur Radiol* 2009; **19**: 1239–45. doi: https://doi.org/10.1007/s00330-008-1264-7
18. Sun Q, Dong MJ, Tao X-feng, Yu Q, Li K-cheng, Yang C. Dynamic MR imaging of temporomandibular joint: an initial assessment with fast imaging employing steady-state acquisition sequence. *Magn Reson Imaging* 2015; **33**: 270–5. doi: https://doi.org/10.1016/j.mri.2014.10.013
19. Kaufman L, Kramer DM, Crooks LE, Ortendahl DA. Measuring signal-to-noise ratios in MR imaging. *Radiology* 1989; **173**: 265–7. doi: https://doi.org/10.1148/radiology.173.1.2781018
20. Henkelman RM. Measurement of signal intensities in the presence of noise in MR images. *Med Phys* 1985; **12**: 232–3. doi: https://doi.org/10.1118/1.595711
21. de Vries M, Nijenhuis RJ, Hoogeveen RM, de Haan MW, van Engelshoven JMA, Leiner T, et al. Contrast-enhanced peripheral MR angiography using SENSE in multiple stations: feasibility study. *J Magn Reson Imaging* 2005; **21**: 37–45. doi: https://doi.org/10.1002/jmri.20240
22. Wintersperger BJ, Runge VM, Biswas J, Reiser MF, Schoenberg SO. Brain tumor enhancement in MR imaging at 3 Tesla: comparison of SNR and CNR gain using TSE and GRE techniques. *Invest Radiol* 2007; **42**: 558–63. doi: https://doi.org/10.1097/RLI.0b013e31803e8b3f
23. Nordmeyer-Massner JA, Wyss M, Andreisek G, Pruessmann KP, Hodler J. In vitro and in vivo comparison of wrist MR imaging at 3.0 and 7.0 Tesla using a gradient echo sequence and identical eight-channel coil array designs. *J Magn Reson Imaging* 2011; **33**: 661–7. doi: https://doi.org/10.1002/jmri.22419
24. Wong OL, Yuan J, Yu SK, Cheung KY. Image quality assessment of a 1.5T dedicated magnetic resonance-simulator for radiotherapy with a flexible radio frequency coil setting using the standard American College of Radiology magnetic resonance imaging phantom test. *Quant Imaging Med Surg* 2017; **7**: 205–14. doi: https://doi.org/10.21037/qims.2017.02.08
25. Kuhn FP, Spinner G, Del Grande F, Wyss M, Piccirelli M, Erni S, et al. MR imaging of the temporomandibular joint: comparison

between acquisitions at 7.0 T using dielectric pads and 3.0 T. *Dentomaxillofac Radiol* 2017; **46**: 20160280. doi: https://doi.org/10.1259/dmfr.20160280

26. Navallas M, Inarejos EJ, Iglesias E, Cho Lee GY, Rodríguez N, Antón J. MR imaging of the temporomandibular joint in juvenile idiopathic arthritis: technique and findings. *Radiographics* 2017; **37**: 595–612. doi: https://doi.org/10.1148/rg.2017160078
27. Laistler E, Poirier-Quinot M, Lambert SA, Dubuisson RM, Girard OM, Moser E, et al. In vivo MR imaging of the human skin at subnanoliter resolution using a superconducting surface coil at 1.5 Tesla. *J Magn Reson Imaging* 2015; **41**: 496–504. doi: https://doi.org/10.1002/jmri.24549
28. Underhill HR, Yarnykh VL, Hatsukami TS, Wang J, Balu N, Hayes CE, et al. Carotid plaque morphology and composition: initial comparison between 1.5- and 3.0-T magnetic field strengths. *Radiology* 2008; **248**: 550–60. doi: https://doi.org/10.1148/radiol.2482071114
29. Erb-Eigner K, Warmuth C, Taupitz M, Willerding G, Bertelmann E, Asbach P. Impact of magnetic field strength and receiver coil in ocular MRI: a phantom and patient study. *Rofo* 2013; **185**: 830–7. doi: https://doi.org/10.1055/s-0033-1335796